

The spherical collapse model and cluster formation beyond the Λ cosmology: Indications for a clustered dark energy?

Spyros Basilakos

Academy of Athens, Research Center for Astronomy and Applied Mathematics, Soranou Efessiou 4, 11527, Athens, Greece

Juan Carlos Bueno Sanchez and Leandros Perivolaropoulos,
Department of Physics, University of Ioannina, Greece

We generalize the small scale dynamics of the universe by taking into account models with an equation of state which evolves with time, and provide a complete formulation of the cluster virialization attempting to address the nonlinear regime of structure formation. In the context of the current dark energy models, we find that galaxy clusters appear to form at $z \sim 1 - 2$, in agreement with previous studies. Also, we investigate thoroughly the evolution of spherical matter perturbations, as the latter decouple from the background expansion and start to “turn around” and finally collapse. Within this framework, we find that the concentration parameter depends on the choice of the considered dark energy (homogeneous or clustered). In particular, if the distribution of the dark energy is clustered then we produce more concentrated structures with respect to the homogeneous dark energy. Finally, comparing the predicted concentration parameter with the observed concentration parameter, measured for four massive galaxy clusters, we find that the scenario which contains a pure homogeneous dark energy is unable to reproduce the data. The situation becomes somewhat better in the case of an inhomogeneous (clustered) dark energy.

PACS numbers: 98.80.-k, 95.35.+d, 95.36.+x

1. INTRODUCTION

Recent studies in observational cosmology lead to the conclusion that the available high quality cosmological data (Type Ia supernovae, CMB, etc.) are well fitted by an emerging “standard model”. This standard model, assuming flatness, is described by the Friedman equation

$$H^2(a) = \left(\frac{\dot{a}}{a}\right)^2 = \frac{8\pi G}{3} [\rho_m(a) + \rho_X(a)] \quad (1.1)$$

where $a(t)$ is the scale factor of the universe, $\rho_m(a)$ is the density corresponding to the sum of baryonic and cold dark matter, with the latter needed to explain clustering, and an extra component $\rho_X(a)$ with negative pressure called dark energy needed to explain the observed accelerated cosmic expansion ([1, 2, 3, 4, 5] and references therein).

The nature of the dark energy is one of the most fundamental and difficult problems in physics and cosmology. Indeed, during the last decade there has been a theoretical debate among the cosmologists regarding the nature of the exotic “dark energy”. Various candidates have been proposed in the literature, such as a cosmological constant Λ (vacuum), time-varying $\Lambda(t)$ cosmologies, quintessence, k -essence, vector fields, phantom, tachyons, Chaplygin gas and the list goes on (see [6, 7, 8, 9, 10, 11, 12, 13, 14, 15, 16, 17, 18, 19, 20] and references therein). Within this framework, high energy field theories generically indicate that the equation of state of such a dark energy is a function of the cosmic time. To identify this type of evolution of the equation of state, a detailed form of the observed $H(a)$ is required which may be obtained by a combination of multiple dark

energy probes.

A serious issue here is how (and when) the large scale structures and in particular galaxy clusters form. Galaxy clusters occupy an eminent position in the structure hierarchy, being the most massive virialized systems known and therefore they appear to be ideal tools for testing theories of structure formation and extracting cosmological information. The cluster distribution basically traces scales that have not yet undergone the non-linear phase of gravitationally clustering, thus simplifying their connections to the initial conditions of cosmic structure formation. In the last decade many authors have been involved in this kind of studies and have found that the main features of the large scale structures (formation epoch, shape etc) can potentially be affected by the dark energy [21, 22, 23, 24, 25, 26, 27, 28, 33, 34, 35, 36, 37, 38, 39, 40].

The aim of this work is along the same lines, attempting to investigate the main properties of the non-linear spherical model for a large family of dark energy models, in which the corresponding equation of state parameter varies as a function of the scale factor of the universe, $w = w(a)$. The plan of the paper is as follows. In section 2 we briefly discuss the dark energy issue. In section 3 we present the various dark energy models and in section 4 we use a joint statistical analysis, in order to place constraints on the main cosmological parameters. Section 5 outlines the theoretical analysis of the spherical collapse model in which the equation of state parameter varies with the cosmic time. In section 6 we present the corresponding theoretical predictions regarding the formation of the galaxy clusters. In section 7, we compare the predicted concentration parameters with those found by four galaxy clusters at relatively large redshifts

$0.18 \leq z \leq 0.45$), using the Subaru 8.3 telescope [81]. Finally, we draw our conclusions in section 8. Throughout the paper we will use $H_0 = 70.5 \text{ km/sec/Mpc}$.

2. THE DARK ENERGY EQUATION OF STATE

In the framework of the general relativity it is well known that for homogeneous and isotropic flat cosmologies, driven by non-relativistic matter and dark energy with equation of state $p_X = w(a)\rho_X$, the expansion rate of the Universe can be written as (see eq.1.1)

$$E^2(a) = \frac{H^2(a)}{H_0^2} = \Omega_m a^{-3} + \Omega_X e^{3 \int_a^1 d \ln y [1+w(y)]} . \quad (2.1)$$

Note, that $E(a)$ is the normalized Hubble flow, Ω_m is the dimensionless matter density at the present epoch, $\Omega_X = 1 - \Omega_m$ is the corresponding dark energy density parameter and $w(a)$ is the dark energy equation of state. Inverting the above equation we simply derive

$$w(a) = \frac{-1 - \frac{2}{3} a \frac{d \ln E}{da}}{1 - \Omega_m a^{-3} E^{-2}(a)} . \quad (2.2)$$

The exact nature of the dark energy has yet to be found and thus the dark energy equation of state parameter includes our ignorance regarding the physical mechanism which leads to a late cosmic acceleration.

On the other hand, it is possible to extent the previous methodology in the framework of modified gravity (see [42, 43]). Instead of using the exact Hubble flow through a modification of the Friedmann equation we can utilize a Hubble flow that looks like the nominal one (see eq.1.1). The key point here is to consider that the accelerated expansion of the universe can be attributed to a “geometrical” dark energy component. Due to the fact that the matter density in the universe (baryonic+dark) can not accelerate the cosmic expansion we perform the following parametrization [42, 43]:

$$E^2(a) = \frac{H^2(a)}{H_0^2} = \Omega_m a^{-3} + \delta H^2 . \quad (2.3)$$

Obviously, with the aid of the latter approach we include any modification to the Friedmann equation of general relativity in the last term of eq.(2.3). Now from eqs.(2.2, 2.3) we can derive, after some algebra, the “geometrical” dark energy equation of state

$$w(a) = -1 - \frac{1}{3} \frac{d \ln \delta H^2}{d \ln a} . \quad (2.4)$$

From now on, for the modified cosmological models we will use the above formulation.

3. LIKELIHOOD ANALYSIS

In this work we use various cosmological observations in order to constrain the dark energy models, explored

here (see section 3). First of all, we use the Baryonic Acoustic Oscillations (BAOs). BAOs are produced by pressure (acoustic) waves in the photon-baryon plasma in the early universe, generated by dark matter overdensities. Evidence of this excess was recently found in the clustering properties of the luminous SDSS red-galaxies [44] and it can provide a “standard ruler” with which we can constraint the dark energy models. In particular, we use the following estimator:

$$A(\mathbf{p}) = \frac{\sqrt{\Omega_m}}{[z_s^2 E(a_s)]^{1/3}} \left[\int_{a_s}^1 \frac{da}{a^2 E(a)} \right]^{2/3} \quad (3.1)$$

measured from the SDSS data to be $A = 0.469 \pm 0.017$, where $z_s = 0.35$ [or $a_s = (1 + z_s)^{-1} \simeq 0.75$] and $E(a) \equiv H(a)/H_0$ is the normalized Hubble flow. Therefore, the corresponding χ_{BAO}^2 function is simply written

$$\chi_{\text{BAO}}^2(\mathbf{p}) = \frac{[A(\mathbf{p}) - 0.469]^2}{0.017^2} \quad (3.2)$$

where \mathbf{p} is a vector containing the cosmological parameters that we want to fit.

On the other hand, a very accurate and deep geometrical probe of dark energy is the angular scale of the sound horizon at the last scattering surface as encoded in the location l_1^{TT} of the first peak of the Cosmic Microwave Background (CMB) temperature perturbation spectrum. This probe is described by the CMB shift parameter [45, 46, 47] which is defined as

$$R = \sqrt{\Omega_m} \int_{a_{ls}}^1 \frac{da}{a^2 E(a)} . \quad (3.3)$$

The shift parameter measured from the WMAP 5-years data [4] to be $R = 1.71 \pm 0.019$ at $z_{ls} = 1090$ [or $a_{ls} = (1 + z_{ls})^{-1} \simeq 9.17 \times 10^{-4}$]. In this case, the χ_{cmb}^2 function is given

$$\chi_{\text{cmb}}^2(\mathbf{p}) = \frac{[R(\mathbf{p}) - 1.71]^2}{0.019^2} \quad (3.4)$$

Finally, we utilize the Union08 sample of 307 supernovae of Kowalski et al. [5]. In this case, the χ_{SNIa}^2 function becomes:

$$\chi_{\text{SNIa}}^2(\mathbf{p}) = \sum_{i=1}^{307} \left[\frac{\mu^{\text{th}}(a_i, \mathbf{p}) - \mu^{\text{obs}}(a_i)}{\sigma_i} \right]^2 . \quad (3.5)$$

where $a_i = (1 + z_i)^{-1}$ is the observed scale factor of the Universe, z_i is the observed redshift, μ is the distance modulus $\mu = m - M = 5 \log d_L + 25$ and $d_L(a, \mathbf{p})$ is the luminosity distance

$$d_L(a, \mathbf{p}) = \frac{c}{a} \int_a^1 \frac{dy}{y^2 H(y)} \quad (3.6)$$

where c is the speed of light. We can combine the above probes by using a joint likelihood analysis:

$$\mathcal{L}_{\text{tot}}(\mathbf{p}) = \mathcal{L}_{\text{BAO}} \times \mathcal{L}_{\text{cmb}} \times \mathcal{L}_{\text{SNIa}}$$

or

$$\chi_{tot}^2(\mathbf{P}) = \chi_{\text{BAO}}^2 + \chi_{\text{cmb}}^2 + \chi_{\text{SNIa}}^2$$

in order to put even further constraints on the parameter space used. Note, that we define the likelihood estimator¹ as: $\mathcal{L}_j \propto \exp[-\chi_j^2/2]$.

4. CONSTRAINTS ON THE FLAT DARK ENERGY MODELS

In this section, we consider a large family of flat dark energy models and with the aid of the above observational data we attempt to put tight constraints on their free parameters. In the following subsections, we briefly present these cosmological models which trace differently the nature of the dark energy.

A. Constant equation of state - QP model

In this case the equation of state is constant (see for a review, [15]; hereafter QP-models). Such dark energy models do not have much physical motivation. In particular, a constant equation of state parameter requires a fine tuning of the potential and kinetic energies of the real scalar field. Despite the latter problem, these dark energy models have been used in the literature due to their simplicity. Notice, that dark energy models with a canonical kinetic term have $-1 \leq w < -1/3$. On the other hand, models of phantom dark energy ($w < -1$) require exotic nature, such as a scalar field with a negative kinetic energy. Now using eq.(2.1) the normalized Hubble parameter becomes

$$E^2(a) = \Omega_m a^{-3} + (1 - \Omega_m) a^{-3(1+w)} . \quad (4.1)$$

Comparing the QP-models with the observational data (we sample $\Omega_m \in [0.1, 1]$ and $w \in [-2, -0.4]$ in steps of 0.01) we find that the best fit values are $\Omega_m = 0.28 \pm 0.02$ and $w = -1.02 \pm 0.06$ with $\chi_{tot}^2(\Omega_m, w)/dof \simeq 309.2/307$ in very good agreement with the 5 years WMAP data [4]. Also Davis et al. [2] using the Essence-SNIa+BAO+CMB and a Bayesian statistics found $\Omega_m = 0.27 \pm 0.04$, while Kowalski et al. [5] utilizing the Union08-SNIa+BAO+CMB obtained $\Omega_m = 0.285_{-0.02-0.01}^{+0.02+0.01}$. Obviously, our results coincide within 1σ errors. It is worth noting that the concordance Λ -cosmology can be described by QP models with w strictly equal to -1. In this case we find: $\Omega_m = 0.28 \pm 0.02$ with $\chi_{tot}^2(\Omega_m)/dof \simeq 309.3/308$.

B. The Braneworld Gravity - BRG model

In the context of a braneworld cosmology (hereafter BRG) the accelerated expansion of the universe can be explained by a modification of gravity in which gravity itself becomes weak at very large distances (close to the Hubble scale) due to the fact that our four dimensional brane survives into an extra dimensional manifold (see [48] and references therein). The interesting point in this scenario is that the corresponding functional form of the normalized Hubble flow, eq. (2.3), is affected only by one free parameter (Ω_m). Notice, that the quantity δH^2 is given by

$$\delta H^2 = 2\Omega_{bw} + 2\sqrt{\Omega_{bw}}\sqrt{\Omega_m a^{-3} + \Omega_{bw}} \quad (4.2)$$

where $\Omega_{bw} = (1 - \Omega_m)^2/4$. The geometrical dark energy equation of state parameter (see eq.2.4) reduces to

$$w(a) = -\frac{1}{1 + \Omega_m(a)} \quad (4.3)$$

where $\Omega_m(a) \equiv \Omega_m a^{-3}/E^2(a)$. The joint likelihood analysis provides a best fit value of $\Omega_m = 0.24 \pm 0.02$, but the fit is rather poor $\chi_{tot}^2(\Omega_m)/dof \simeq 369/308$.

C. The parametric Dark Energy - CPL model

In this model we utilize the Chevalier-Polarski-Linder ([49, 50], hereafter CPL) parametrization. The dark energy equation of state parameter is defined as a first order Taylor expansion around the present epoch:

$$w(a) = w_0 + w_1(1 - a) . \quad (4.4)$$

The normalized Hubble parameter is given by (see eq.2.1):

$$E^2(a) = \Omega_m a^{-3} + (1 - \Omega_m) a^{-3(1+w_0+w_1)} e^{3w_1(a-1)} \quad (4.5)$$

where w_0 and w_1 are constants. We sample the unknown parameters as follows: $w_0 \in [-2, -0.4]$ and $w_1 \in [-2.6, 2.6]$. We find that for the prior of $\Omega_m = 0.28$ the overall likelihood function peaks at $w_0 = -1.1_{-0.16}^{+0.22}$ and $w_1 = 0.60_{-1.54}^{+0.62}$ while the corresponding $\chi_{tot}^2(w_0, w_1)/dof$ is 307.6/307.

D. The low Ricci dark energy - LRDE model

In this modified cosmological model, we use a simple parametrization for the Ricci scalar which is based on a Taylor expansion around the present time: $\mathcal{R} = r_0 + r_1(1 - a)$ [for more details see [43]]. It is interesting to mention that at the early epochs the cosmic evolution tends asymptotically to be matter dominated. In this framework, we have

$$E^2(a) = \begin{cases} a^{4(r_0+r_1-1)} e^{4r_1(1-a)} & a \geq a_t \\ \Omega_m a^{-3} & a < a_t \end{cases} \quad (4.6)$$

¹ Likelihoods are normalized to their maximum values. Note, that the step of sampling is 0.01 and the errors of the fitted parameters represent 2σ uncertainties. Note that the overall number of data points used is $N_{tot} = 309$ and the degrees of freedom: $dof = N_{tot} - n_{fit}$, with n_{fit} the number of fitted parameters, which vary for the different models.

where $a_t = 1 - (1 - 4r_0)/4r_1$. The matter density parameter at the present epoch, is directly related with the above constants via

$$\Omega_m = \left(\frac{4r_0 - 4r_1 - 1}{4r_1} \right)^{4r_0 + 4r_1 - 1} e^{1 - 4r_0} . \quad (4.7)$$

The corresponding equation of state parameter is given by

$$w(a) = \frac{1 - 4\mathcal{R}}{3} \left[1 - \Omega_m e^{-\int_a^1 (1 - 4\mathcal{R})(dy/y)} \right]^{-1} . \quad (4.8)$$

Notice, that we sample the unknown parameters as follows: $r_0 \in [0.5, 1.5]$ and $r_1 \in [-2.4, -0.1]$ and here are the results: $r_0 = 0.82 \pm 0.04$ and $r_1 = -0.74_{-0.08}^{+0.10}$ ($\Omega_m \simeq 0.28$) with $\chi_{tot}^2(r_0, r_1)/dof \simeq 309.8/307$.

E. The high Ricci dark energy - HRDE model

A different than the previously mentioned geometrical method was proposed by Linder [51], in which the Ricci scalar at high redshifts evolves as

$$\mathcal{R} \simeq \frac{1}{4} \left[1 - 3w_1 \frac{\delta H^2}{H^2} \right] \quad (4.9)$$

where $\delta H^2 = E^2(a) - \Omega_m a^{-3}$. In this geometrical model the normalized Hubble flow becomes:

$$E^2(a) = \Omega_m a^{-3} (1 + \beta a^{-3w_1})^{-\ln \Omega_m / \ln(1 + \beta)} \quad (4.10)$$

where $\beta = \Omega_m^{-1} - 1$. Using the same sampling as in the QP-models, the joint likelihood peaks at $\Omega_m = 0.28 \pm 0.03$ and $w_1 = -1.02 \pm 0.1$ with $\chi_{tot}^2(\Omega_m, w_1)/dof \simeq 309.2/307$. To this end, the effective equation of state parameter is related to $E(a)$ according to eq.(2.2).

F. The tension of cosmological magnetic fields - TCM model

Recently, [52] proposed a novel idea which is based on the following consideration (hereafter TCM): if the cosmic magnetic field is generated in sources (such as galaxy clusters) whose overall dimensions remain unchanged during the expansion of the Universe, the stretching of this field by the cosmic expansion generates a tension (negative pressure) that could possibly explain a small fraction of the dark energy ($\sim 5 - 10\%$). In this flat cosmological scenario the normalized Hubble flow becomes:

$$E^2(a) = \Omega_m a^{-3} + \Omega_\Lambda + \Omega_B a^{-3+n} \quad (4.11)$$

where Ω_B is the density parameter for the cosmic magnetic fields and $\Omega_\Lambda = 1 - \Omega_m - \Omega_B$. The equation of state parameter which is related to magnetic tension is (see eq.2.1)

$$w(a) = -\frac{3\Omega_\Lambda + n\Omega_B a^{-3+n}}{3(\Omega_\Lambda + \Omega_B a^{-3+n})} . \quad (4.12)$$

To this end, we sample $\Omega_B \in [0, 0.3]$ and $n \in [0, 10]$ and we find that for the prior of $\Omega_m = 0.28$ the best fit values are: $\Omega_B = 0.10 \pm 0.10$ and $n = 3.60_{-2.60}^{+4.5}$ with $\chi_{tot}^2(\Omega_B, n)/dof \simeq 308.9/307$.

G. The Pseudo-Nambu Goldstone boson - PNGB model

In this cosmological model the dark energy equation of state parameter is expressed with the aid the potential $V(\phi) \propto [1 + \cos(\phi/F)]$ [54]:

$$w(a) = -1 + (1 + w_0)a^F \quad (4.13)$$

where $w_0 \in [-2, -0.4]$ and $F \in [0, 8]$. Obviously, for $a \ll 1$ we get $w(a) \rightarrow -1$. Based on this parametrization the normalized Hubble function is given by

$$E^2(a) = \Omega_m a^{-3} + (1 - \Omega_m)\rho_X(a) . \quad (4.14)$$

In this context, the corresponding equation of state parameter is

$$\rho_X(a) = \exp \left[\frac{3(1 + w_0)}{F} (1 - a^F) \right] . \quad (4.15)$$

Notice, that the likelihood function peaks at $w_0 = -1.04 \pm 0.17$ and $F = 5.9 \pm 3.2$ with $\chi_{tot}^2(w_0, F)/dof \simeq 317/307$.

H. The early dark energy - EDE model

Another cosmological scenario that we include in our paper is the early dark energy model (hereafter EDE). The basic assumption here is that at early epochs the amount of dark energy is not negligible [55]. In this framework, the overall dark energy component is given by

$$\Omega_X(a) = \frac{1 - \Omega_m - \Omega_e(1 - a^{-3w_0})}{1 - \Omega_m - \Omega_m a^{3w_0}} + \Omega_e(1 - a^{-3w_0}) \quad (4.16)$$

where Ω_e is the early dark energy density and w_0 is the equation of state parameter at the present epoch. Notice, that the EDE model was designed to simultaneously (a) mimic the effects of the late dark energy and (b) provide a decelerated expansion of the universe at high redshifts. The normalized Hubble parameter is written as

$$E^2(a) = \frac{\Omega_m a^{-3}}{1 - \Omega_X(a)} \quad (4.17)$$

while using eq.(2.2), we can obtain the equation of state parameter as a function of the scale factor. Now, from the joint likelihood analysis we find that $\Omega_e = 0.05 \pm 0.04$ and $w_0 = -1.14_{-0.10}^{+0.18}$ (for the prior of $\Omega_m = 0.28$) with $\chi_{tot}^2(\Omega_e, w_0)/dof \simeq 308.7/307$.

I. The Variable Chaplygin Gas - VCG model

Let us consider now a completely different model namely the variable Chaplygin gas (hereafter VCG) which corresponds to a Born-Infeld tachyon action [56, 57]. Recently, an interesting family of Chaplygin gas models was found to be consistent with the current observational data [58]. In the framework of a spatially flat geometry, it can be shown that the normalized Hubble function takes the following formula:

$$E^2(a) = \Omega_b a^{-3} + (1 - \Omega_b) \sqrt{B_s a^{-6} + (1 - B_s) a^{-n}} \quad (4.18)$$

where $\Omega_b \simeq 0.021 h^{-2}$ is the density parameter for the baryonic matter [59] and $B_s \in [0.01, 0.51]$ and $n \in [-4, 4]$. The effective matter density parameter is: $\Omega_m^{eff} = \Omega_b + (1 - \Omega_b) \sqrt{B_s}$. We find that the best fit parameters are $B_s = 0.05 \pm 0.02$ and $n = 1.58^{+0.35}_{-0.43}$ ($\Omega_m^{eff} \simeq 0.26$) with $\chi_{tot}^2(B_s, n)/dof \simeq 314.7/307$.

5. EVOLUTION OF MATTER PERTURBATIONS

In this section we study the spherical collapse model by generalizing the basic non-linear equations which govern the behavior of the matter perturbations within the framework of the previously described dark energy models. Also, we compare our predictions with the traditional Λ cosmology. This can help us to understand better the theoretical expectations of the current dark energy models as well as the variants from the concordance Λ cosmology.

A. The Evolution of the linear growth factor

The evolution equation of the growth factor for models where the dark energy fluid has a vanishing anisotropic stress and the matter fluid is not coupled to other matter species is given by ([42], [60], [61], [62]):

$$D'' + \frac{3}{2} \left[1 - \frac{w(a)}{1 + X(a)} \right] \frac{D'}{a} - \frac{3}{2} \frac{X(a)}{1 + X(a)} \frac{D}{a^2} = 0 \quad (5.1)$$

where

$$X(a) = \frac{\Omega_m}{1 - \Omega_m} e^{-3 \int_a^1 w(y) d \ln y} = \frac{\Omega_m a^{-3}}{\delta H^2} . \quad (5.2)$$

Note, that the prime denotes derivatives with respect to the scale factor. Useful expressions of the growth factor can be found for the Λ CDM cosmology in [60], for dark energy models with $w = const$ in [63], [22], [25], [64], for dark energy models with a time varying equation of state in [65] and for the scalar tensor models in [66]. Finally, in this work, the growth factor evolution for the current cosmological model is derived by solving numerically eq. (5.1). Note, that the growth factors are normalized to unity at the present time.

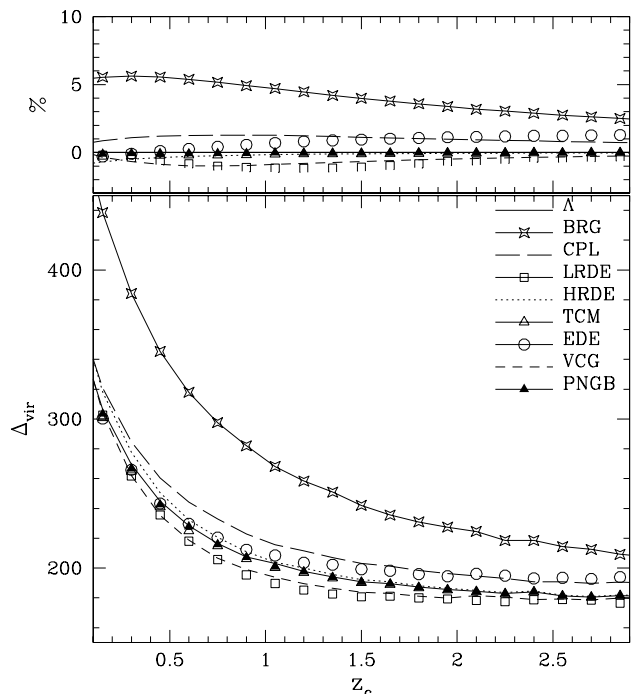


FIG. 1: *Upper Panel:* The deviation $(1 - \lambda_X/\lambda_\Lambda)\%$ of the collapse factor for various dark energy models with respect to the Λ solution (solid line). *Bottom Panel:* The density contrast at the virialization, Δ_{vir} , as a function of redshift. The points represent the following cosmological models: (a) BRG (open stars), (b) LRDE (open squares), (c) TCM (open triangles), (d) EDE (open circles) and (e) PNGB (solid triangles). The lines represent: (a) CPL model (long dashed), (b) HRDE model (dot line) and VCG model (dashed line).

B. The spherical collapse model

The spherical collapse model, which has a long history in cosmology, is a simple but still a fundamental tool for understanding how a small spherical patch [with radius $R(t)$] of homogeneous overdensity forms a bound system via gravitational instability [67]. From now on, we will call a_t the scale factor of the universe where the overdensity reaches its maximum expansion ($\dot{R} = 0$) and a_c the scale factor in which the sphere virializes implying that a large scale structure has formed, while R_t and R_c are the corresponding radii of the spherical overdensity. Note that in the spherical region, $\rho_{ms} \propto R^{-3}$ is the matter density, ρ_m is the background matter density and ρ_{Xs} denotes the corresponding density of the dark energy. In order to address the issue of how the dark energy itself affects the gravitationally bound systems (clusters of galaxies), we have to deal with the following situations: (i) clustered dark energy, considering that the whole system virializes (both matter and dark energy), (ii) the dark energy remains clustered but now only the matter virializes and (iii) the dark energy remains homogeneous and only the corresponding matter virializes (for more

TABLE I: Numerical results. The 1st column indicates the dark energy model used. Between column two and four, we present the main properties of the spherical collapse model, assuming that galaxy clusters have formed prior to the epoch of $a_c \sim 0.42$ ($z_c \sim 1.4$), in which the most distant cluster has been found [68]. Column five, corresponds to the current age of the universe, t_0 . Finally, the last two rows correspond to the (γ_1, n_1) constants which are included in the approximate $\Delta_{vir}(a)$ formula (see eq.5.16).

Model	z_{ta}	Δ_{vir}	ζ	t_0/Gyr	γ_1	n_1
Λ	2.89	192.0	5.56	13.72	0	0
QP	2.89	191.3	5.55	13.77	0.384	2.350
BRG	2.98	247.3	5.89	13.40	0.446	-0.556
CPL	2.90	204.6	5.66	13.62	0.210	-1.40
LRDE	2.86	181.2	5.49	13.84	0.152	-6.848
HRDE	2.89	193.6	5.63	13.77	0.050	-0.117
TCM	2.89	191.4	5.56	13.78	0.450	5.387
PNGB	2.89	191.9	5.57	13.76	0	0
EDE	2.88	200.1	5.71	13.71	0.054	-1.70
VCG	2.85	185.1	5.53	14.01	0.226	-1.245

details see [28], [35] [39] and [40]). Note, that in this section we are using the third possibility (for more on inhomogeneous dark energy see section 7B).

In this section, we review only some basic concepts of the problem based on the assumption that the dark energy component under a scale of galaxy clusters can be treated as being homogeneous: $\rho_{X_s}(a) = \rho_X(a)$ and $w_s(a) = w(a)$. In general the evolution of the spherical perturbations as the latter decouple from the background expansion is given by the Raychaudhuri equation:

$$\frac{\ddot{R}}{R} = -\frac{4\pi G}{3}[\rho_{ms} + \rho_{X_s}(1 + 3w_c)] . \quad (5.3)$$

Now, if we perform the transformations

$$x = \frac{a}{a_t} \quad \text{and} \quad y = \frac{R}{R_t} , \quad (5.4)$$

then eqs.(1.1, 5.3) become:

$$\dot{x}^2 = H_t^2 \Omega_{m,t} [\Omega_m(x)x]^{-1} \quad (5.5)$$

and

$$\ddot{y} = -\frac{H_t^2 \Omega_{m,t}}{2} \left[\frac{\zeta}{y^2} + \nu y I(x, y) \right] \quad (5.6)$$

with

$$\nu = \frac{\rho_{X,t}}{\rho_{m,t}} = \frac{1 - \Omega_{m,t}}{\Omega_{m,t}} \quad (5.7)$$

where $\rho_{X,t}$ is the dark energy density at the turn around epoch and $\Omega_{m,t}$ is the corresponding matter density parameter. Also, $\rho_{ms,t} = \zeta \rho_{m,t}$ is the matter density for the spherical region at the turn around time, while $\rho_{m,t}$ denotes the background matter density at the same epoch.

Note, that in order to obtain the above set of equations which govern the global and local dynamics, we have utilized the following relations:

$$\rho_{ms} = \rho_{ms,t} \left(\frac{R}{R_t} \right)^{-3} = \frac{\zeta \rho_{m,t}}{y^3} \quad (5.8)$$

and

$$I(x, y) = I(x) = [1 + 3w(x)] f(x) \quad (5.9)$$

where

$$f(x) = e^{3 \int_x^1 d \ln u [1+w(u)]} . \quad (5.10)$$

Finally, $\Omega_m(x)$ is given by

$$\Omega_m(x) = \frac{1}{1 + \nu x^3 f(x)} . \quad (5.11)$$

In this context, the time needed for a spherical shell to re-collapse is twice the turn-around time, $t_f \simeq 2t_t$ which implies

$$\int_0^{a_c} \frac{1}{H(a)a} da = 2 \int_0^{a_t} \frac{1}{H(a)a} da . \quad (5.12)$$

In the case of the usual Λ cosmology one can prove that

$$\sinh^{-1} \left(a_c^{3/2} \sqrt{\nu_0} \right) = 2 \sinh^{-1} \left(a_t^{3/2} \sqrt{\nu_0} \right) \quad (5.13)$$

where $\nu_0 = (1 - \Omega_m)/\Omega_m$. Of course, in order to include the dark energy models in our analysis we have to solve eq.(5.12) numerically. As an example, assuming that galaxy clusters have formed prior to the epoch of $a_c \sim 0.42$ ($z_c \sim 1.4$), in which the most distant cluster has been found [68], the turn around epoch is not really affected by the dark energy component (see Table 1), ie. $a_t \sim 0.26$ (or $z_t \sim 2.8$). This is to be expected, due to the fact that at large redshifts matter dominates the Hubble expansion. It is worth noting that the ratio between the scale factors converges to the Einstein de Sitter ($\Omega_m = 1$) value $\left(\frac{a_c}{a_t} \right) = 2^{2/3}$ at high redshifts which implies that $\zeta \simeq \left(\frac{3\pi}{4} \right)^2$.

On the other hand, utilizing both the virial theorem and the energy conservation² we reach to the following condition:

$$\left[\frac{1}{2} R \frac{\partial}{\partial R} (U_G + U_{X_s}) + U_G + U_{X_s} \right]^{a=a_c} = [U_G + U_{X_s}]^{a=a_t} \quad (5.14)$$

² In fact, a smooth dark energy component violates the energy conservation, in the sense that the dark energy freely flows outwards the overdensity [28, 39]. Only small scale clustering dark energy would satisfy the energy conservation, for instance the chameleon models [29, 30, 31, 32]. Such violation is however only important at very late times, when dark energy dominates.

where $U_G = -3GM^2/5R$ is the potential energy and $U_{X_s} = -4\pi GM(1+3w)\rho_{X_s}R^2/5$ is the potential energy associated with the dark energy for the spherical overdensity (see [28] and [35]). Using the above formulation we can obtain a cubic equation that relates the ratio between the virial R_c and the turn-around outer radius R_t the collapse factor ($\lambda = R_c/R_t$). Of course in the case of $w = -1$ the above expressions get the usual form for Λ cosmology ([25], [21]) while for an Einstein-de Sitter model ($\Omega_m = 1$) we have $\lambda = 1/2$.

Finally solving numerically eq.(5.14) we calculate the collapse factor. In general, we find that the collapse factor lies in the range $0.43 \leq \lambda \leq 0.50$ in agreement with previous studies ([25], [28], [35], [39], [33], [37], [40]). Also, in the upper panel of figure 1 we plot the deviation, $(1 - \lambda_X/\lambda_\Lambda)\%$, of the collapse factors $\lambda_X(z_c)$ for the current dark energy models with respect to the Λ solution $\lambda_\Lambda(z_c)$. It becomes evident that the shape of the cosmic structures which produced by the CPL (long dashed line), LRDE (open squares), HRDE (dot line), TCM (open triangles) and PNGB (solid triangles) models is close to that predicted by the usual Λ cosmology. On the other hand, the largest positive deviation of the collapse factor occurs for the BRG model (open stars) which implies that the latter model produces more bound systems with respect to the above dark energy models. Therefore, within this cosmological scenario the corresponding large scale structures should locate in very large density environments. The opposite situation holds for the VCG (dashed line) and LRDE (open squares) models due to their negative deviations.

In the bottom panel of figure 1 we present the evolution of the density contrast at virialization

$$\Delta_{vir} = \frac{\rho_{ms,c}}{\rho_{m,c}} = \frac{\zeta}{\lambda^3} \left(\frac{a_c}{a_t} \right)^3 \quad (5.15)$$

where $\rho_{ms,c}$ is the matter density in the virialized structure while $\rho_{m,c}$ is the background matter density at the same epoch. We verify, that the density contrast decreases with the formation (virialization) redshift z_c . Obviously, the factor Δ_{vir} , provided by the spherical collapse model, plays a key role in this kind of studies. Indeed, the differences among the Δ_{vir} for the current dark energy models enter through the $H(z)$ (see eq. (5.12)). This feature implies that perhaps the density contrast at virialization can be used as a cosmological tool (see section 7). In any case, at very large redshifts the above density contrast tends to the Einstein-de Sitter value ($\Delta_{vir} \sim 18\pi^2$), as it should. In this context, following the notations of [27, 69, 70], we provide an accurate fitting formula to Δ_{vir} (within a physical range of cosmological parameters)

$$\Delta_{vir} = 18\pi^2 [1 + \gamma \Theta^n(a)] \quad (5.16)$$

where

$$\gamma = 0.44 - 1.31(|w(a_*)|^{n_1} - 1)$$

$$n = 0.94 - 0.21(|w(a_*)|^{n_1} - 1)$$

$a_* = 0.4$ (or $z_* = 1.5$) and $\Theta(a) = \Omega_m^{-1}(a) - 1$. Note, that γ_1 and n_1 are constants (see the last rows of Table1).

Finally, in Table 1 we list the results of the spherical collapse model considering that galaxy clusters have formed at $z_c \sim 1.4$, ie., (a) the cosmological models and the value of the turn around redshift, (b) the virial density Δ_{vir} , at the collapse time, as well as the density excess of the matter density in the spherical overdensity, ζ , at the turn around time, (c) the predicted age of the universe and (d) the constants (γ_1, n_1) which are included in eq.(5.16).

6. THE FORMATION OF GALAXY CLUSTERS

In this section we briefly investigate the cluster formation processes by generalizing the basic equations which govern the behavior of the matter perturbations within the framework of the current dark energy models. Also we compare our predictions with those found for the traditional Λ cosmology. This can help us to understand better the theoretical expectations of the dark energy models as well as the variants from the usual Λ cosmology.

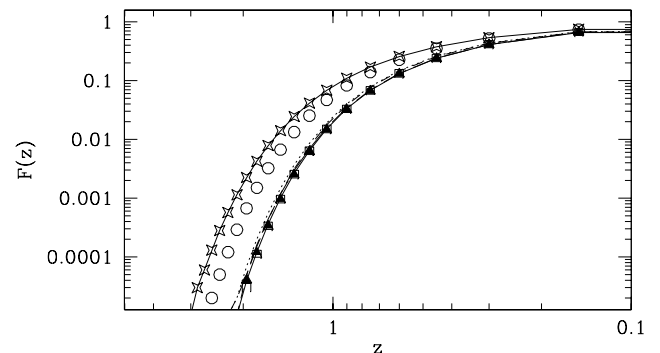


FIG. 2: The predicted fractional rate of cluster formation as a function of redshift for the current cosmological models ($\sigma_8 = 0.80$).

The concept of estimating the fractional rate of cluster formation has been brought up by different authors [71, 72]. In particular, these authors introduced a methodology which computes the rate at which mass joins virialized structures, which grow from small initial perturbations in the universe. In particular, the basic tool is the Press-Schechter formalism [73] which considers the fraction of mass in the universe contained in gravitationally bound structures (such as galaxy clusters) with matter fluctuations greater than a critical value δ_c , [74]. Assuming that the density contrast is normally distributed with zero mean and variance $\sigma^2(M, z)$ we have:

$$\mathcal{P}(\delta, z) = \frac{1}{\sqrt{2\pi}\sigma(M, z)} \exp \left[-\frac{\delta^2}{2\sigma^2(M, z)} \right]. \quad (6.1)$$

In this kind of studies it is common to parametrize the rms mass fluctuation amplitude at $8 h^{-1}\text{Mpc}$ which can be expressed as a function of redshift as $\sigma(M, z) = \sigma_8(z) = D(z)\sigma_8$. The current cosmological models are normalized by the analysis of the WMAP 5 years data $\sigma_8 = 0.80$ [4]. The integration of eq.(6.1) provides the fraction of the universe, on some specific mass scale, that has already collapsed producing cosmic structures (galaxy clusters) at redshift z and is given by [72]:

$$P(z) = \int_{\delta_c}^{\infty} \mathcal{P}(\delta, z) d\delta \quad (6.2)$$

or

$$P(z) = \frac{1}{2} \left[1 - \text{erf} \left(\frac{\delta_c}{\sqrt{2}\sigma_8(z)} \right) \right] \quad (6.3)$$

where δ_c is the linearly extrapolated density threshold above which structures collapse, [74]. Notice, that for the model of modified gravity (BRG) we use $\delta_c \simeq 1.47$ (see [75]), for the EDE model we use $\delta_c \simeq 1.4$ (see [76] and references therein). To this end, for the rest of the dark energy models, due to the fact that $w \simeq -1$ close to the present epoch, we utilize a δ_c approximation which is given by Weinberg & Kamionkowski (see [27], their eq.18).

Obviously the above generic of form eq.(6.3) depends on the choice of the background cosmology. The next step is to normalize the probability to give the number of clusters which have already collapsed by the epoch z (cumulative distribution), divided by the number of clusters which have collapsed at the present epoch ($z = 0$), $F(z) = P(z)/P(0)$. In figure 2 we present in a logarithmic scale the behavior of normalized cluster formation rate as a function of redshift for the present dark energy models. In general, prior to $z \sim 0.2$ the cluster formation has terminated due to the fact that the matter fluctuation field, $D(z)$, effectively freezes. For the traditional Λ cosmology we find the known behavior in which galaxy clusters appear to be formed at high redshifts $z \sim 2$ (see for example [25] and references therein). From figure 2 it becomes also clear, that the vast majority of the dark energy models seem to have a cluster formation rate which is close to that predicted by the usual Λ cosmology (see solid line in figure 2). However, for the BRG and EDE cosmological scenarios respectively we find that galaxy clusters appear to form earlier ($z \sim 3$) with respect to the CPL, LRDE, HRDE, TCM, PNGB and VCG dark energy models.

7. COMPARISON WITH OBSERVATIONS

A. Homogeneous Dark energy

A useful observable parameter that is predictable in the context of the spherical collapse model is the concentration parameter c_{vir} . This parameter characterizes

the profile of cluster dark matter halo which in turn is usually modelled by the NFW profile [77, 78] defined as

$$\rho_{NFW}(R) = \frac{\rho_s}{(R/r_s)(1 + R/r_s)^2} \quad (7.1)$$

where r_s and ρ_s are the characteristic radius and density of the halo profile. The concentration parameter c_{vir} is an observable characteristic of the halo profile and is defined as $c_{vir} = r_{vir}/r_s$ where r_{vir} is the virial radius of the system [77, 78, 79]. Dark matter profiles of clusters may be determined using lens distortion and magnification [41, 80]. Such profiles have been recently obtained [41] for four clusters using the wide-field camera Suprime-Cam [81] of the Subaru 8.3m telescope. The NFW profile fits well the profile of these clusters and the concentration parameters have been obtained for all four clusters [41].

The theoretical prediction of the concentration parameter for each cluster can be made using the results of the previous section in the context of the spherical collapse model with any dark energy parametrization assuming homogeneity of dark energy. In what follows we consider the CPL parametrization of equation (4.4). In particular, we use the approach of Ref. [82] (see also [83]) to obtain the predicted value of the concentration parameter from the density contrast at virialization Δ_{vir} . This is a simple effective algorithm that approximates well the values of the concentration parameter obtained from N-body simulations in the context of various cosmological dark energy models including the case of the cosmological constant. In this approach, the concentration parameter c_{vir} is related to $\Delta_{vir}(z)$ as³

$$c_{vir}^3 = \frac{\Delta_{vir}(z_c) \Omega_m(z_0)(1 + z_c)^3}{\Delta_{vir}(z_0) \Omega_m(z_c)(1 + z_0)^3} \quad (7.2)$$

where z_c is the formation (virialization) redshift while z_0 is the ‘‘observed’’ redshift ($z = z_0 \leq z_c$). The formation redshift z_c may be obtained [82] from the relation

$$D(z_c)\sigma_{eff}(M) = \frac{1}{C_\sigma} \quad (7.3)$$

where $D(z)$ is the linear growth factor and $\sigma_{eff}(M)$ is the *effective* amplitude of the power spectrum on a scale M connected with the actual amplitude on a scale M by

$$\sigma_{eff}(M) = \sigma(M) \left[-\frac{d \ln \sigma}{d \ln M}(M) \right] \quad (7.4)$$

C_σ is a constant with $C_\sigma \simeq 28$ [82]. The power spectrum amplitude $\sigma(M)$ is well approximated by the fit [84]

$$\sigma(M) = \sigma_8 \left(\frac{M}{M_8} \right)^{-\gamma_1(M)/3} \quad (7.5)$$

³ Note that Δ_{vir} entering Eq. (7.2) is defined with respect to the critical density ρ_{crit} [82], rather than with respect to $\rho_{m,c}$ as in Eq. (5.15). Computing c_{vir} then requires to multiply Δ_{vir} in Eqs. (5.15) and (5.16) by $\rho_{m,c}/\rho_{crit}$.

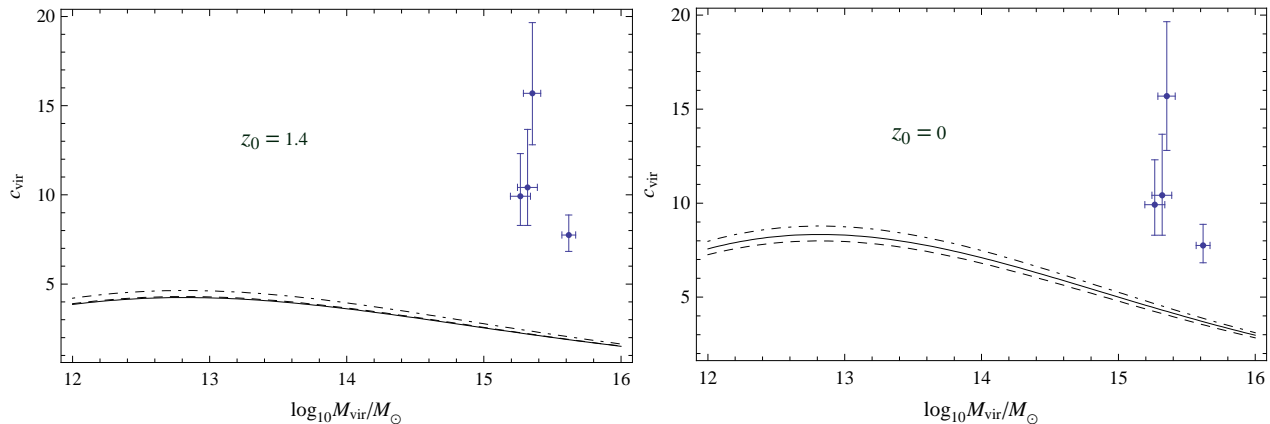


FIG. 3: a: The concentration parameter $c_{vir}(M_{vir})$ for homogeneous dark energy for $(w_0, w_1) = (-1, 0)$ (Λ CDM) (solid line), $(w_0, w_1) = (-1.1, 0.6)$ (best fit of section 4C) and $(w_0, w_1) = (-0.6, 0)$ (dot-dashed line). For comparison we include the predicted curve (dashed line) for the values at which the overall likelihood function peaks: $(w_0, w_1) = (-1.1, 0.6)$ (see Sec. 4). Redshift $z_0 = 1.4$ has been assumed. b: Same as Fig. 3a with $z_0 = 0$.

where $M_8 = 6 \times 10^{14} \Omega_{0m} h^{-1} M_\odot$ is the mass inside a sphere of radius $R_8 = 8h^{-1} \text{Mpc}$. Also

$$\gamma_1(M) = (0.3\Gamma + 0.2) \left[2.92 + \frac{1}{3} \log\left(\frac{M}{M_8}\right) \right] \quad (7.6)$$

with $\Gamma = \Omega_{0m} h e^{-\Omega_b - \Omega_b/\Omega_{0m}}$ ($\Omega_b = 0.05$ is the baryonic density parameter). The linear growth function in equation (7.3) is obtained as (eg [85])

$$D(z) = e^{\int_1^{1/(1+z)} \Omega_m(a)^\gamma \frac{da}{a}} \quad (7.7)$$

where γ is the effective growth index which depends mildly on the dark energy properties in the observationally allowed parameter range ($\gamma = 0.55$ for Λ CDM).

Using equations (7.3), (7.5), (7.6) and the parametrization (5.16) to evaluate $\Delta_{vir}(z)$ we may use equation (7.2) to evaluate $c_{vir}(M_{vir})$ for various values of redshift z_0 and compare with the corresponding data of Ref. [41]. The results are shown in Fig. 3a for $z_0 = 1.4$ and in Fig. 3b for $z_0 = 0$. In both cases we consider $(w_0, w_1) = (-1, 0)$ (Λ CDM) and $(w_0, w_1) = (-0.6, 0)$ which slightly improves the fit to the data of Ref. [41] shown in the same figures (values $w_0 < -1$ further decrease the quality of fit). We have also tested other cases with $w_1 \neq 0$ and we have found that the value of c_{vir} depends (mildly) only on the *mean value* of $w(z)$ at late times when dark energy begins to dominate.

The results shown in Fig. 3 correspond to homogeneous dark energy and confirm the well known puzzle for Λ CDM namely that the predicted concentration parameter in this model is significantly less than the observed one [41]. The new input of Fig. 3 is that the modification of dark energy evolution (within the observationally allowed range) is unable to resolve this puzzle if homogeneity is assumed for dark energy. As discussed in the next subsection however the agreement with observations can improve significantly if dark energy is assumed to cluster along with the non-linearly clustered dark matter.

B. Inhomogeneous Dark energy

Although it has been shown that the dark energy fluid does not cluster on scales smaller than 100Mpc [86], it is also interesting to consider the case when the dark energy clusters along with the dark matter. Such a behavior is expected in models of interacting dark energy with dark matter and may also be a result of the gravitational interaction between nonlinearly clustered dark matter and dark energy. In the inhomogeneous case, the dark energy component flows progressively out of the overdensity [35, 36], and hence energy conservation cannot be applied to determine the collapse factor λ (along with the virial theorem). In order to simplify the inhomogeneous formalism, we consider the extreme case in which the dark energy fully clusters along with the dark matter and thus we avoid the energy non-conservation problem examined in Ref. [35]. The merit of this assumption is that it allows an analytical solution to the system of Eqs. (5.5) and (5.6) [40] due to the fact that the function $I(x, y)$ in eq.(5.6) depends only on y

$$I(x, y) = I(y) = [1 + 3w(R(y))] \frac{f(R(y))}{f(\alpha_t)}. \quad (7.8)$$

Therefore, the solution of the system is

$$\int_0^1 \left[\frac{y}{\zeta + \nu y P(y) - (\zeta + P(1)\nu)y} \right]^{1/2} dy = \int_0^1 [x \Omega_m(x)]^{1/2} dx \quad (7.9)$$

where $P(y) = y^2 f(R(y))/f(a_t)$ and $R(y) = \zeta^{-1/3} a_t y$. The matter contrast ζ can be obtained by solving numerically the above equation.

Although the dark energy clusters, it may not take part in the virialization process, in which case the collapse

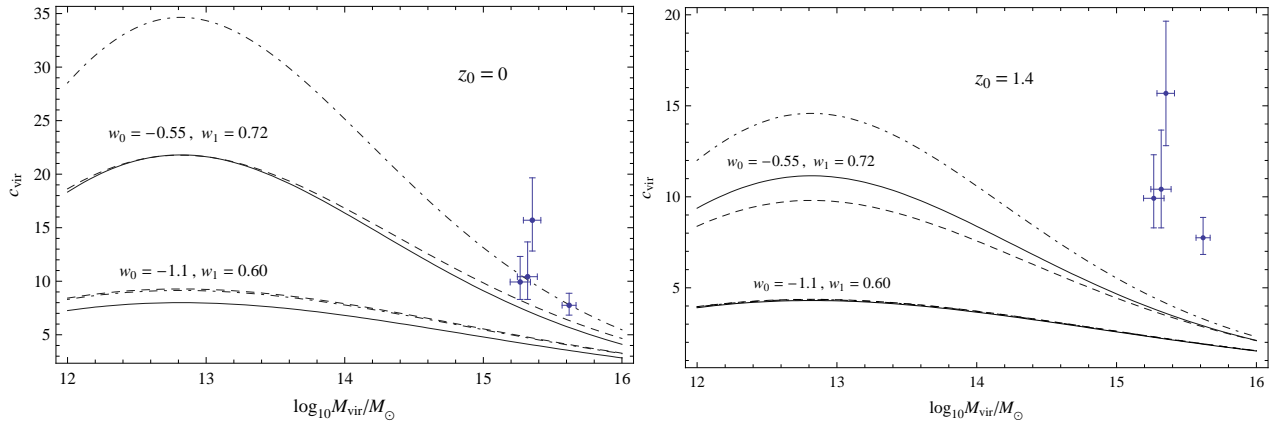


FIG. 4: a: Concentration parameter $c_{vir}(M_{vir})$ for the inhomogeneous dark energy when only matter virializes (dashed line) and when both matter and quintessence virialize (dot-dashed line) with $z_0 = 0$. We include the homogeneous case (solid line) for comparison. The three upper curves correspond to $(w_0, w_1) = (-0.55, 0.72)$, whereas the three bottom ones correspond to the values where the overall likelihood function peaks: $(w_0, w_1) = (-1.1, 0.60)$. b: Same as Fig. 4a with $z_0 = 1.4$.

factor is determined by eq. (5.14). However, if the dark energy participates in the virialization, the self-energy of the dark energy must also be taken into account. In such a case, the equation that determines the collapse factor is [35]

$$\left[\frac{1}{2} R \frac{\partial U_{tot}}{\partial R} + U_{tot} \right]^{a=a_c} = [U_{tot}]^{a=a_t}, \quad (7.10)$$

where

$$U_{tot} = \frac{1}{2} \int (\rho_m + \rho_{Xs})(\Phi_m + \Phi_{Xs}) dV,$$

and Φ_m and Φ_{Xs} are the gravitational potentials of the matter and dark energy components for a spherical overdensity.

After solving for ζ and λ we use eq. (5.12) to compute Δ_{vir} from eq. (5.15) at different redshifts, and then c_{vir} from eq. (7.2). It was noted in Ref. [36] that the c_{vir} corresponding to inhomogeneous dark energy models may be larger than the corresponding to their homogeneous realizations, although such enhancement in c_{vir} is model dependent. Such an increase in c_{vir} owes primarily to the factor $\Delta_{vir}(z_c)/\Delta_{vir}(z_0)$ in eq. (7.2), and it is shown in [36] that for certain models this factor may be significantly larger than 1. For example, the inhomogeneous realization of the model in Ref. [11] results in a c_{vir} that can be larger by a factor of 2.

In the CPL model we find that, in general, although c_{vir} may be somewhat larger in the inhomogeneous case, this improvement is insufficient to account for observations if the dark energy component is sub-dominant at the time of turn-around. The situation improves when we allow the dark energy to give a non-negligible contribution at turn-around, which can be arranged by taking $w_1 \gtrsim w_0$ (see Fig 4). As mentioned before, in such a case energy conservation cannot be used to determine the collapse factor. However, it is interesting to examine

the predictions for c_{vir} obtained by pretending that energy is conserved, hence using eqs. (5.14) and (7.10) to determine λ . Of course, in this case one must understand c_{vir} as an estimate to its actual value.

Assuming then energy conservation to estimate λ , we begin by the case when only the matter component virializes. In that case $\Delta_{vir}(z_c)/\Delta_{vir}(z_0)$ in eq. (7.2) is of order 1, and so the enhancement factor in c_{vir} is lost. We find that in the range of M_{vir} of interest to observations: $10^{15} M_\odot \lesssim M_{vir} \lesssim 10^{16} M_\odot$ [41], the concentration parameter behaves roughly as $c_{vir} \sim \frac{1+z_c}{1+z_0}$. The agreement with observations then depends almost exclusively on z_0 and z_c , requiring an early rapid collapse of the halo subunits: $z_c \sim 7$ for $z_0 \simeq 0$. The agreement with observations ameliorates if the dark energy component also virializes. The reason is that in such a case the corresponding collapse factor is smaller than if only matter virializes [40]. Consequently, the factor $\Delta_{vir}(z_c)/\Delta_{vir}(z_0)$ increases, becoming significantly larger than 1 in the observational range of M_{vir} provided w_1 is properly tuned (see Fig. 4). Similar results to the ones presented in Fig. 4 may be obtained for a wide range of values of w_0 (assuming of course w_1 is conveniently tuned), in particular for $w_0 \simeq -1$, which is in better agreement with current observations. In Fig.4.b we present the results for c_{vir} for $z_0 = 1.4$. In this case, the factor $\Delta_{vir}(z_c)/\Delta_{vir}(z_0)$ is counteracted by the term $\frac{1+z_c}{1+z_0}$, and hence agreement with observations cannot be attained in this case.

To conclude we would like to emphasize that the results presented in Fig. 4, owing to the aforementioned energy non-conservation problem, must be understood as an estimate to the actual value of c_{vir} . A more reliable estimate for c_{vir} must obviously account for energy non-conservation in the equation determining the collapse factor λ . As pointed out in [39], taking this effect into account results in a further reduction of the collapse factor λ . Therefore, one can expect that a more

detailed study will place c_{vir} in better agreement with observations.

8. CONCLUSIONS

In this paper we study analytically and numerically the spherical collapse model beyond the usual Λ cosmology, by using several parameterizations for the dark energy equation of state. In this framework, we first perform a joint likelihood analysis in order to put tight constraints on the main cosmological parameters by using the current observational data (SNIa, CMB shift parameter and BAOs). For the vast majority of the dark energy models, we find that the large scale structures (such as galaxy clusters) start to form prior to $z \sim 1 - 2$ [40, 72]. The amplitude and the shape of the concentration parameter (c_{vir}) is affected by the considered status of the dark energy model (homogeneous or clustered). We verify that in the case where the distribution of the dark energy is clustered we are producing more concentrated struc-

tures with respect to the homogeneous dark energy. Finally, we go a step further by comparing the predicted concentration parameters with those observed for four massive galaxy clusters ($0.18 \leq z \leq 0.45$) and we find that the homogeneous dark energy pattern is unable to reproduce the data. The situation becomes somewhat better in the case of an inhomogeneous (clustered) dark energy. In order to confirm such a possibility, we need to create robust cluster surveys at relatively high redshifts ($1.5 \geq z \geq 0.2$). The latter result points to the direction that perhaps the c_{vir} parameter can be used in the future in order to understand the physical properties of the dark energy.

Acknowledgments

We would like to thank David Mota for his useful comments and suggestions. This work was supported by the European Research and Training Network MRTPN-CT-2006 035863-1 (UniverseNet).

-
- [1] A. G. Riess, *et al.*, *Astrophys. J.*, **659**, 98, (2007)
 - [2] W.M. Wood-Vasey *et al.*, *Astrophys. J.*, **666**, 694, (2007); T.M. Davis *et al.*, *Astrophys. J.*, **666**, 716, (2007)
 - [3] D.N. Spergel, *et al.*, *Astrophys. J. Suplem.*, **170**, 377, (2007)
 - [4] E. Komatsu, *et al.*, *Astrophys. J. Suplem.*, **180**, 330, 2009
 - [5] M. Kowalski, *et al.*, *Astrophys. J.*, **686**, 749, (2008)
 - [6] B. Ratra, P. J. Peebles, *Phys. Rev. D.*, **37**, 3406, (1988)
 - [7] M. Ozer M. and O. Taha, *Nucl. Phys.*, **B287**, 776, (1987)
 - [8] S. Weinberg, *Rev. Mod. Phys.*, **61**, 1, (1989)
 - [9] C. Wetterich, *Astron. Astrophys.* **301**, 321 (1995)
 - [10] R. R. Caldwell, R. Dave, P. J. Steinhardt, *Phys. Rev. Lett.*, **80**, 1582, (1998)
 - [11] P. Brax, J. Martin, *Phys. Lett.* **B468**, 40 (1999)
 - [12] A. Kamenshchik, U. Moschella, V. Pasquier, *Phys. Lett. B.*, **511**, 265, (2001)
 - [13] A. Feinstein, *Phys. Rev. D.*, **66**, 063511, (2002)
 - [14] R.R., Caldwell, E. V., *Phys. Rev. Lett.*, **545**, 23, (2002)
 - [15] P. J. Peebles, B. Ratra, *Rev. Mod. Phys.*, **75**, 559, (2003)
 - [16] L. P. Chimento, A. Feinstein, *Mod. Phys. Lett. A*, **19**, 761, (2004)
 - [17] A. W. Brookfield, C. van de Bruck, D. F. Mota, D. Tocchini-Valentini, *Phys. Rev. Lett.* **96**, 061301 (2006)
 - [18] E. J. Copeland, M. Sami, S. Tsujikawa, *Int. J. Mod. Phys. D*, **15**, 1753 (2006)
 - [19] C. G. Boehmer, T. Harko, *Eur. Phys. J.* **C50**, 423 (2007)
 - [20] J. Frieman, M. Turner, D. Huterer, *Annual Rev. of Astron. and Astrop.*, **46**, 385, (2008)
 - [21] O. Lahav, P. B. Lilje, J. R. Primack, &, M. J. Rees, *Mon. Not. Roy. Astron. Soc.*, **251**, 128, (1991)
 - [22] L. Wang, & J. P. Steinhardt, *Astrophys. J.*, **508**, 483, (1998)
 - [23] I. T. Iliev, &, P. R. Shapiro, *Mon. Not. Roy. Astron. Soc.*, **325**, 468, (2001)
 - [24] R. A. Battye, &, J. Weller, *Phys. Rev. D*, **68**, 3506, (2003)
 - [25] S. Basilakos, *Astrophys. J.*, **590**, 636, (2003)
 - [26] M. Manera and D. F. Mota, *Mon. Not. Roy. Astron. Soc.* **371**, 1373 (2006)
 - [27] N. N., Weinberg, &, M. Kamionkowski, *Astrophys. J.*, **341**, 251, (2003)
 - [28] D. F. Mota &, C. van de Bruck C., *Astronomy & Astrophysics*, **421**, 71, (2004)
 - [29] P. Brax, C. van de Bruck, A. C. Davis, J. Khoury and A. Weltman, *Phys. Rev. D* **70**, 123518 (2004)
 - [30] D. F. Mota and J. D. Barrow, *Mon. Not. Roy. Astron. Soc.* **349**, 291 (2004)
 - [31] P. Brax, C. van de Bruck, A. C. Davis and A. M. Green, *Phys. Lett. B* **633**, 441 (2006)
 - [32] D. F. Mota and D. J. Shaw, *Phys. Rev. D* **75**, 063501 (2007)
 - [33] C. Horellou & J. Berge, *Mon. Not. Roy. Astron. Soc.*, **360**, 1393, (2005)
 - [34] Ding-fang Zeng, &, Yi-hong Gao, 2005, (astro-ph/0505164)
 - [35] I. Maor, &, O. Lahav, *Journal of Cosmology and Astroparticle Physics*, **7**, 3, (2005)
 - [36] David F. Mota *JCAP* **09**, 006 (2008)
 - [37] W. J. Percival, *Astronomy & Astrophysics*, **443**, 819, (2005)
 - [38] N. J. Nunes, &, D. F. Mota, *Mon. Not. Roy. Astron. Soc.*, **368**, 751, (2006)
 - [39] P. Wang, *Astrophys. J.*, **640**, 18, (2006)
 - [40] S. Basilakos, &, N. Voglis, *Mon. Not. Roy. Astron. Soc.*, **374**, 269, (2007)
 - [41] T. Broadhurst, K. Umetsu, E. Medezinski, M. Oguri and Y. Rephaeli, *Astrophys. J.* **685**, L9 (2008) [arXiv:0805.2617 [astro-ph]].
 - [42] E. V. Linder and A. Jenkins, *Mon. Not. Roy. Astron. Soc.*, **346**, 573, (2003)
 - [43] E. V. Linder, *Phys. Rev. Lett.* **70**, 023511, (2004); E. V. Linder, *Rep. Prog. Phys.*, **71**, 056901, (2008)
 - [44] D. J. Eisenstein D. J., *et al.*, *Astrophys. J.*, **633**, 560,

- (2005); N. Padmanabhan, et al., *Mon. Not. Roy. Astron. Soc.*, **378**, 852, (2007)
- [45] J. R. Bond, G. Efstathiou and M. Tegmark, *Mon. Not. Roy. Astron. Soc.* **291**, L33, (1997)
- [46] R. Trotta, [arXiv:astro-ph/0410115].
- [47] S. Nesseris, & L. Perivolaropoulos, *JCAP* **0701**, 018, (2007)
- [48] C. Deffayet, G. Dvali, & G. Cabadadze, *Phys. Rev. D.*, **65**, 044023, (2002)
- [49] M. Chevallier and D. Polarski, *Int. J. Mod. Phys. D* **10**, 213, (2001)
- [50] E. V. Linder, *Phys. Rev. Lett.* **90**, 091301, (2003)
- [51] E. V. Linder, & R. N. Cahn, *Astrop. Phys.*, **28**, 481, (2007)
- [52] I. Contopoulos, & S. Basilakos, *Astron. Astrophys.* **471**, 59, (2007)
- [53] U. Alam, V. Sahni, T. D. Saini, A. A. Starobinsky, *Mon. Not. Roy. Astron. Soc.*, **344**, 1057, (2003)
- [54] J. A. Frieman, C.T Hill, A. Stebbins, I. Waga, *Phys. Rev. Lett.*, **75**, 2077, (1995); K. Dutta, & L. Sorbo, *Phys. Rev. D.*, **75**, 063514, (2007); A. Abrahamse, A. Albrecht, M. Bernard, B. Bozek, *Phys. Rev. D.*, **77**, 103504, (2008)
- [55] I. Zlatev, L. Wang, P. J. Steinhardt, *Phys. Rev. Lett.*, **82**, 896, (1999); M. Doran, S. Stern, E. Thommes, *JCAP*, **0704**, 015, (2006)
- [56] M. C. Bento, O. Bertolami, A. A. Sen, *Phys. Rev. D.*, **70**, 083519, (2004)
- [57] Z. K. Guo, & Y. Z., Zhang, astro-ph/0506091, (2005); Z. K. Guo, & Y. Z., Zhang, astro-ph/050979, (2005)
- [58] M. Makler, S. Q. de Oliveira, I. Waga, *Phys. Lett. B.*, **555**, 1, (2003); M. C. Bento, O. Bertolami, A. A. Sen, *Phys. Lett. B.*, **575**, 172, (2003); A. Dev, J. S. Alcaniz, D. Jain, *Phys. Rev. D.*, **67**, 023515, (2003); Y. Gong, C. K. Duan, *Mon. Not. Roy. Astron. Soc.*, **352**, 847, (2004); Z. H. Zhu, *Astron. Astrophys.*, **423**, 421, (2004) L. Amendola, I. Waga, F. Finelli, astro-ph/0509099;
- [59] D. Kirkman, D. Tytler, N. Suzuki, N., J. M. O'Meara, D. Lubin, *Astrophys. J. Suppl.*, *ApJS*, **149**, 1, (2003)
- [60] P. J. E. Peebles, 1993, *Principles of Physical Cosmology*, Princeton University Press, Princeton New Jersey, (1993)
- [61] F. H. Stabenau, & B. Jain, *Phys. Rev. D*, **74**, 084007, (2006)
- [62] P. J. Uzan, *Gen. Rel. Grav.*, **39**, 307, (2007)
- [63] V. Silveira, & I. Waga, *Phys. Rev. D.*, **64**, 4890, (1994)
- [64] S. Nesseris & L. Perivolaropoulos, *Phys. Rev. D.*, **77**, 3504, (2008)
- [65] V. E. Linder & N. R. Cahn, *Astroparticle Physics*, **28**, 481, (2007)
- [66] R. Gannouji, & D. Polarski, (2008), [arXiv:0802.4196]
- [67] J. E. Gunn, & J. R. Gott, *Astrophys. J.*, **176**, 1, (1972)
- [68] C. R. Mullis, P. Rosati, G. Lamer, H. Böehringer, P. Schuecker & R. Fassbender, *Mon. Not. Roy. Astron. Soc.*, **623**, L85, (2005); S. A. Stanford, et al., *Astrophys. J.*, **646**, L13, (2006)
- [69] T. Kitayama, & Y. Suto, **469**, 480, (1996)
- [70] Douglas J. Shaw, David F. Mota, *Astrophys.J.Suppl.*, **174**, 277, (2008).
- [71] P. J. E. Peebles, *Astrophys. J.*, **284**, 439, (1984); S. Weinberg, **59**, 2607, (1987);
- [72] D. Richstone, A. Loeb & E. L. Turner, *Astrophys. J.*, **393**, 477, (1992)
- [73] W. H. Press and P. Schechter, *Astrophys. J.* **187**, 425 (1974).
- [74] V. Eke, S. Cole & C. S. Frenk, *Mon. Not. Roy. Astron. Soc.*, **282**, 263, (1996)
- [75] B. M. Schafer, & K. Koyama, *Mon. Not. Roy. Astron. Soc.*, **385**, 411, (2008)
- [76] M. Bartelmann, M. Doran, C. Wetterich, *Astron. & Astrophys.*, **454**, 27, (2006)
- [77] J. F. Navarro, C. S. Frenk and S. D. M. White, *Astrophys. J.* **462**, 563 (1996) [arXiv:astro-ph/9508025].
- [78] J. F. Navarro, C. S. Frenk and S. D. M. White, *Astrophys. J.* **490**, 493 (1997) [arXiv:astro-ph/9611107]
- [79] R. H. Wechsler, J. S. Bullock, J. R. Primack, A. V. Kravtsov and A. Dekel, *Astrophys. J.* **568**, 52 (2002) [arXiv:astro-ph/0108151].
- [80] K. Umetsu and T. Broadhurst, *Astrophys. J.* **684**, 177 (2008) [arXiv:0712.3441]
- [81] S. Miyazaki *et al.*, arXiv:astro-ph/0211006.
- [82] V. R. Eke, J. F. Navarro and M. Steinmetz, *Astrophys. J.* **554**, 114 (2001) [arXiv:astro-ph/0012337].
- [83] D. F. Mota, [arXiv:0812.4493 [astro-ph]].
- [84] L. Liberato and R. Rosenfeld, *JCAP* **0607**, 009 (2006) [arXiv:astro-ph/0604071].
- [85] S. Nesseris and L. Perivolaropoulos, *Phys. Rev. D* **77**, 023504 (2008) [arXiv:0710.1092 [astro-ph]].
- [86] R. Dave, R. R. Caldwell and P. J. Steinhardt, *Phys. Rev. D* **66** (2002) 023516 [arXiv:astro-ph/0206372].